

Effect of exciton self-trapping and molecular conformation on photophysical properties of oligofluorenes

Stefan Schumacher,¹ Arvydas Ruseckas,² Neil A. Montgomery,² Peter J. Skabara,³ Alexander L. Kanibolotsky,³ Martin J. Paterson,⁴ Ian Galbraith,¹ Graham A. Turnbull,² and Ifor D. W. Samuel^{2,a)}

¹*Department of Physics, School of Engineering and Physical Sciences, SUPA, Heriot-Watt University, Edinburgh EH14 4AS, United Kingdom*

²*Organic Semiconductor Centre, School of Physics and Astronomy, SUPA, University of St. Andrews, North Haugh, St. Andrews, Fife KY16 9SS, United Kingdom*

³*WestCHEM, Department of Pure and Applied Chemistry, University of Strathclyde, Glasgow G1 1XL, United Kingdom*

⁴*Department of Chemistry, School of Engineering and Physical Sciences, Heriot-Watt University, Edinburgh EH14 4AS, United Kingdom*

(Received 6 April 2009; accepted 17 September 2009; published online 21 October 2009)

Electronic absorption and fluorescence transitions in fluorene oligomers of differing lengths are studied experimentally and using density functional theory (DFT) and time-dependent DFT. Experimental values are determined in two ways: from the measured molar absorption coefficient and from the radiative rate deduced from a combination of fluorescence quantum yield and lifetime measurements. Good agreement between the calculated and measured transition dipoles is achieved. In both theory and experiment a gradual increase in transition dipoles with increasing oligomer length is found. In absorption the transition dipole follows an $\sim n^{0.5}$ dependence on the number of fluorene units n for the range of $2 \leq n \leq 12$, whereas a clear saturation of the transition dipole with oligomer length is found in fluorescence. This behavior is attributed to structural relaxation of the molecules in the excited state leading to localization of the excitation (exciton self-trapping) in the middle of the oligomer for both twisted and planar backbone conformations. Twisted oligofluorene chains were found to adopt straight or bent geometries depending on alternation of the dihedral angle between adjacent fluorene units. These different molecular conformations show the same values for the transition energies and the magnitude of the transition dipole. © 2009 American Institute of Physics. [doi:10.1063/1.3244984]

I. INTRODUCTION

Conjugated polymers show attractive optical and electrical properties for applications in optoelectronic devices. Among them, polyfluorenes are efficient blue emitters,^{1–5} also showing ambipolar charge transport⁶ and strong two-photon absorption.^{7,8} Their application in light emitting diodes,^{2–5} field effect transistors,^{9,10} polymer lasers,^{11–14} and optical amplifiers¹⁵ has been demonstrated. Polyfluorenes can form liquid crystalline phases, which can be aligned on oriented substrates and show highly polarized fluorescence.^{4,16,17} Films with a controlled fraction of a planar conformation (so called β -phase) can be prepared by spin coating from solutions using different additives, by exposing the prepared films to solvent vapors or by thermal treatment.^{18–21} This phase shows a better photochemical stability,^{22,23} faster charge transport,²⁴ and could have advantages in polymer laser applications.²⁵ Despite the vast technological interest in this material and its photophysical properties, the microscopic understanding of excitations is still not complete. The effective conjugation length in polyfluorene has been estimated to be about 12 fluorene units,²⁶ whereas the extent of the excited state delocalization found by theoretical studies is

only about three repeat units.²⁷ Previous theoretical and experimental studies of oligofluorenes with up to seven repeat units showed a clear convergence of transition energies and a linear dependence of the oscillator strength on the oligomer length in absorption.^{27–31} Experimental reports did not include the data on the fluorescence quantum yield (QY),^{29–31} which are needed to determine the trend in the oscillator strength of fluorescence transitions.

In this paper we study the dependence of the transition dipoles and transition energies on oligomer length in a family of fluorene oligomers. Transition dipoles in absorption are determined from the molar absorption coefficient and in fluorescence from the fluorescence lifetime and QY. Transition energies and transition dipoles for both twisted and planar conformations are in good agreement with values obtained using time-dependent density functional theory (DFT) calculations. We studied the increase in transition dipole with increasing oligomer length. We found that the increase in transition dipole deduced from fluorescence saturates at shorter oligomer lengths than that deduced from absorption. This result can be explained by exciton self-trapping after excitation.

The conformations of fluorene oligomers are also studied theoretically for oligomers with up to 12 repeat units. We

^{a)}Electronic mail: idws@st-and.ac.uk.

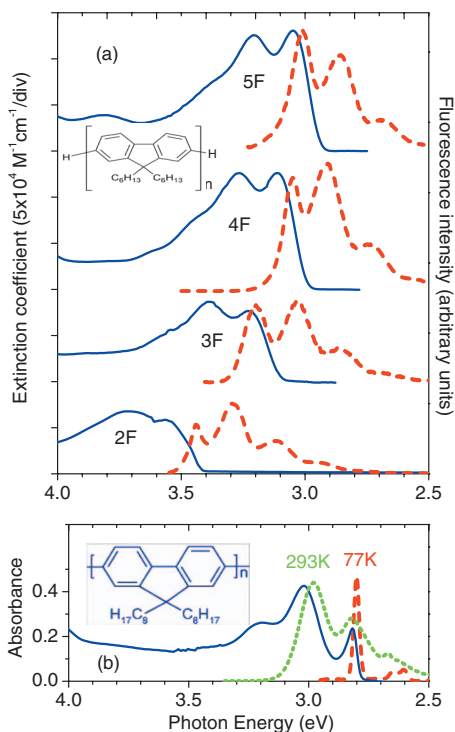


FIG. 1. (a) Molar extinction coefficient (solid lines) and fluorescence (dashed lines) spectra of the fluorene oligomers with n fluorene units (nF) in 2MeTHF at 77 K. Excitation was at the peak of absorption. Spectra are offset vertically for clarity. Panel (b) shows absorption spectrum of PFO in 2MeTHF at 77 K (solid line) and fluorescence spectra at 77 K (dashed line) and at 293 K (dotted line). Chemical structures are shown in the insets.

show that fluorene oligomers can adopt significantly different molecular conformations depending on the way the fluorene repeat units are twisted. In addition to the obtained insight into exciton self-trapping and conformational disorder of oligofluorenes, we also report on experimental and theoretical results for the planar (β -phase) conformation and on DFT calculations using periodic boundary conditions (PBCs) mimicking the fluorene polymers.

The remainder of this paper is organized as follows. In Sec. II we introduce the experimental and theoretical methods used in this work. Section III contains the results and discussion. It starts with a comparison of experimental and theoretical data for fluorene oligomers and a polymer in the twisted (also called the α -phase) and in the planar conformation (β -phase). Based on additional theoretical data, this is followed by a discussion of excitation self-trapping in the excited state relaxed geometry, and different possible molecular conformations of the oligomers. We conclude with a discussion of theoretical data obtained from PBC calculations.

II. METHODS

In this study we used fluorene oligomers functionalized with two hexyl side groups per repeat unit [structure is shown in Fig. 1(a)] and poly(9,9-dioctylfluorenyl-2,7-diyl) (PFO) [Fig. 1(b)]. Oligofluorenes with up to four repeat units were synthesized using the previously described method.³² Fluorene pentamer and PFO, which is end capped with dimethylphenyl, were obtained from American Dye Source Inc.

and were used as received. Solutions were prepared in anhydrous 2-methyltetrahydrofuran (2MeTHF), which was obtained from Sigma-Aldrich. Spectroscopic experiments were performed in 1 cm fused silica cuvettes, and the absorbance of the samples was less than 1. Frozen solutions at 77 K were measured in an Oxford Optistat DN liquid nitrogen cryostat using helium exchange gas.

Absorption and fluorescence spectra were recorded on a Cary spectrophotometer and JY Horiba Fluoromax 2 fluorimeter, respectively. Fluorescence QY was measured at room temperature using quinine sulfate in 0.5M sulfuric acid (fluorescence QY of 0.51) as a reference. Fluorescence lifetimes in all oligomers were measured with a streak camera with a 3 ps time resolution using 100 fs pulses at 380 nm for excitation, except for the monomer, for which excitation was at 266 nm.

Absorption transition dipoles $|d_a|$ in units of Debye have been determined using the measured molar decadic absorption coefficient $\epsilon(\tilde{\nu})$ integrated over the absorption band,³³

$$|d_a|^2 = 9.186 \times 10^{-3} n_0 \int [\epsilon(\tilde{\nu})/\tilde{\nu}] d\tilde{\nu}, \quad (1)$$

where $\tilde{\nu}$ is the frequency of the transition in cm^{-1} and n_0 is the refractive index of the medium (in this case the solvent). We used the spectrum of $\epsilon(\tilde{\nu})$ measured in 2 MeTHF at 77 K for all oligomers except the monomer, for which the room temperature spectrum was used. Shrinkage of the solution volume by 3% with the temperature decrease from 293 to 77 K was taken into account when calculating the molar extinction coefficient at low temperature.³⁴ Transition dipoles in fluorescence are determined as detailed below in Sec. III A.

We carried out DFT and time-dependent DFT (TD-DFT) calculations to determine equilibrium geometries, vertical transition energies, and transition dipoles of the fluorene oligomer molecules under investigation. For these calculations, the GAUSSIAN03 package was used. All the data in this work were calculated using the B3LYP functional together with the 6-31G basis set, only the CIS excited state geometry optimizations were done using the smaller 3-21G basis set to allow for the treatment of oligomer chains containing up to 12 fluorene units, much longer than previously studied.^{27,28} The CIS calculations have been performed with the frozen core option. The computational accuracy achieved using the B3LYP functional together with the above choice of basis sets has been shown to yield ground and excited state properties such as molecular geometries and transition energies of oligofluorenes that are in good agreement with available experimental data.^{28,35} Unless otherwise noted, all calculations in the present work have been done for oligomers with finite and alternating dihedral angles between adjacent fluorene units.

For the fluorene monomer, dimer, and trimer we tested the influence of additional polarization functions in the basis set. For the ground state equilibrium geometry (optimized with 6-31G*) of the monomer, dimer, and trimer, the lowest singlet transition energy with 6-31G* is reduced by 0.5%, 1.6%, and 1.7%, respectively, compared to the 6-31G result, and the corresponding transition dipole is increased by 0.2% and 0.4% for the monomer and trimer, respectively, and re-

duced by 0.16% for the dimer. These results confirm earlier findings²⁸ that additional polarization functions in the basis set do not seem to play a crucial role for the molecules studied.

III. RESULTS AND DISCUSSION

A. Transition dipoles and transition energies

The absorption and fluorescence spectra of the oligomers are shown in Fig. 1(a). All spectra show vibronic peaks spaced by ~ 0.16 eV, which is a characteristic energy of the vibrational modes of the carbon-carbon bonds and is generally observed in conjugated polymers. When oligomer length increases, the spectra shift to the red and the 0-0 vibronic transition becomes dominant. The molar absorption coefficient increases by about 10% at the peak when the temperature is decreased from 293 to 77 K, which can be explained by reduction in conformational disorder at low temperature. The 0-0 transition energies and spectra are similar to those reported previously.³⁰ The absorption spectrum of the frozen solution of the polymer [Fig. 1(b)] shows a 0-0 peak at 3 eV and a vibronic progression to higher energies as in the earlier report,³⁰ and it also shows an additional peak at 2.82 eV, which is not observed at room temperature. The position of this low energy peak agrees very well with the 0-0 transition of the β -phase conformation previously reported in films¹⁷⁻²¹ and in a poor solvent.³⁶ The polymer fluorescence spectrum at 77K shows a narrow 0-0 peak at 2.8 eV, which is characteristic of the β -phase conformation and two 0-1 peaks, which are redshifted by 0.15 and 0.19 eV relative to the 0-0 peak and attributed to stretching modes of single and double carbon-carbon bonds, respectively. The room temperature fluorescence spectrum peaks at 2.98 eV and corresponds to the twisted backbone conformation. Our observation of the redshifted absorption and fluorescence peaks in a frozen solution, which are characteristic of the β -phase optical transitions, suggest that the planar backbone conformation can form in isolated conjugated chains under the strain imposed by the solidification of the matrix. It is consistent with recent experimental reports of the formation of the planar backbone conformation in the short-chain oligomers dispersed in poly-(methyl methacrylate) matrix²¹ and in polyfluorene chains on the single molecule level in the zeonex matrix.^{22,23} This suggests that the results obtained on isolated conjugated chains with the planar backbone conformation can be used to understand the photophysical properties of the β phase in the neat films.

In Fig. 2 we show different sets of measured data for the lowest optically active electronic transition in a series of oligofluorenes in solution. Time-resolved fluorescence measurements gave decays that were monoexponential and independent of the detection energy. There is a clear trend of decreasing lifetime with increasing oligomer length. The measured fluorescence QY increases with the length of the oligomers and saturates at about 0.8 for the longest oligomers and PFO. To make these measured data comparable to theoretical data obtained from TD-DFT calculations on single molecules, the next step is to determine how the transition dipole changes with the oligomer length. In an earlier

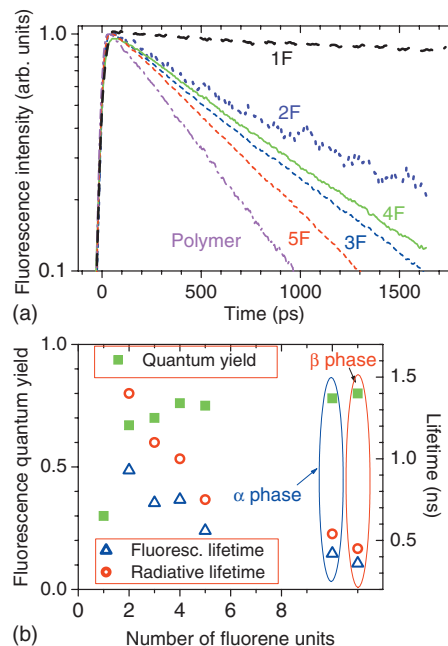


FIG. 2. (a) Fluorescence decays of oligofluorenes and PFO in solution at room temperature. (b) Fluorescence QY and lifetime measured in oligomers and in the different phases of PFO. Oligomer and α -phase data are at room temperature, the β -phase data are in frozen solution at 77 K.

study this has been done directly by calculating the transition dipoles from the measured lifetimes,²⁸ however, this is not sufficient as the transition dipole is a function of both the fluorescence QY and lifetime. Here, the transition dipole in fluorescence $|d_f|$ has been determined using^{33,37}

$$|d_f|^2 = \frac{3\pi\epsilon_0\hbar^4 c^3 \langle E^{-3} \rangle}{n_0 \tau_R}, \quad (2)$$

where $\langle E^{-3} \rangle = \int E^{-3} I(E) dE / \int I(E) dE$ is obtained from the fluorescence intensity $I(E)$ in units of the relative number of quanta at the photon energy E , ϵ_0 is the vacuum dielectric constant, $\hbar = h/2\pi$ is Planck's constant, c is speed of light, and τ_R is the radiative lifetime, which is obtained from the measured fluorescence QY and fluorescence lifetime τ_f using

$$\tau_R = \tau_f / QY. \quad (3)$$

The QY values vary for the different oligomers, which leads to distinctive differences between the fluorescence lifetime and the radiative lifetime of the oligomers. Therefore, it is obvious that experimentally the dependence of the transition dipole on the oligomer length cannot be determined accurately from the fluorescence lifetime alone.^{28,31}

In Fig. 3(a) we compare the experimentally determined and calculated transition dipoles. A strong increase in transition dipole both in absorption and emission with oligomer length is found in experiment and theory. Taking the finite fluorescence QY into account in determining the transition dipole in fluorescence, we find very good agreement between theory and experiment in absolute numbers (much better agreement than reported earlier).²⁸ We note that our theoretical results show small (and insignificant) deviations from the calculated data in Ref. 28, which is due to the slightly smaller basis set used. Absorption dipoles are by about 20%

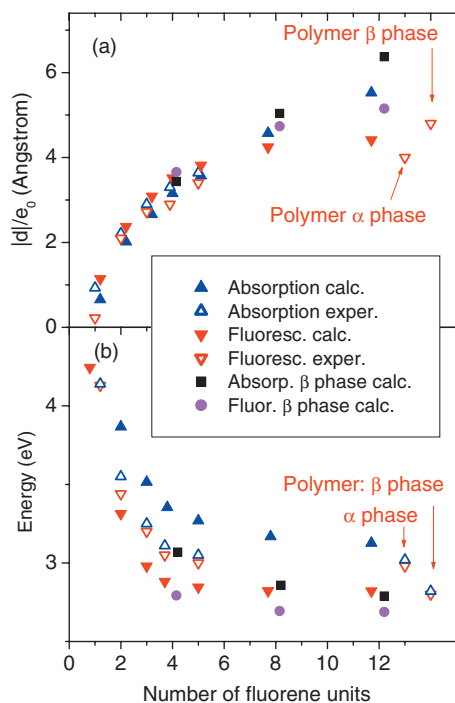


FIG. 3. (a) and (b) show experimental (open symbols) and calculated (solid symbols) transition dipoles, d , and the 0-0 transition energies. The arrows indicate the experimental data in PFO for glassy (α -phase) and planar (β -phase) conformations. All experimental values are obtained at 77 K, except for fluorescence dipoles of the oligomers and of the polymer in α -phase, which are at 293 K. Calculated energies are vertical electronic transition energies in S_0 and S_1 equilibrium geometries, respectively.

higher than the previously reported experimental values for oligofluorenes with up to seven repeat units,³¹ the origin of this difference is currently unknown. Fluorescence dipoles of the planar backbone conformation are within 10% of the reported values in ladder-type oligo-*para*-phenylenes for the same number of benzene rings (two rings per fluorene repeat

unit),³⁸ which indicates that the photophysical properties of these two materials are similar. To deepen the insight obtained from the present work, in the calculations, we extended the series of studied oligomers to much longer oligomers than experimentally and previously theoretically studied containing up to 12 fluorene repeat units. Based on these extended calculations, in the following, we are able to address physical aspects (the existence of different molecular conformations, exciton self-trapping and its role in the saturation of transition dipoles with increasing oligomer length) that are important to the photophysics of oligo- and polyfluorenes, and which have not been discussed and were not accessible in previous work.²⁸ The data are summarized in Table I together with the experimental data.

In Fig. 3(b) experimental and calculated transition energies are given. Here the experimental transition energies represent the spectral position of the 0-0 vibronic peak in absorption and fluorescence. The calculated energies are the vertical transition energies E_{vert} for the equilibrium geometries of the S_0 and S_1 electronic states. In all the different sets of data a clear decrease in transition energy with increasing oligomer length is visible which appears to converge to a constant value, when the oligomer length increases. Convergence is already visible in the pentamer ($n=5$) with longer oligomer chains showing only a slight decrease in the transition energy. It is interesting to compare this with the convergence of transition energies in oligo-*para*-phenylenes, oligophenylenevinyls, and oligothiophenes, which is generally observed at the length of 18–22 double bonds along the shortest path of the conjugated backbone (see the review paper of Gierschner *et al.*).³⁹ As the fluorene pentamer has 20 double bonds along the shortest path of the conjugated backbone, similar behavior is found as for other oligomers of this class.

TABLE I. Vertical transition energies E_{vert} , transition dipoles $|d|$, radiative lifetime τ_{rad} , and energies of the 0-0 vibronic transitions E_{0-0} obtained from experiment and theoretical calculations.

Oligomer length		E_{vert} (eV)		Trans. dipole $ d /e_0$ (Å)		E_{0-0} (eV)		τ_{rad} (ns)
		Abs.	Em.	Abs.	Em.	Abs.	Em.	
1	Experiment	4.64	3.91	0.9	0.22	4.09	4.07	23
	Theory	4.70	4.24	0.7	1.1
2	Experiment	3.82	3.23	2.2	2.1	3.55	3.44	1.4
	Theory	3.86	3.31	2.0	2.4
3	Experiment	3.49	2.99	2.9	2.7	3.25	3.20	1.1
	Theory	3.51	2.98	2.7	3.1
4	Experiment	3.34	2.88	3.3	2.9	3.11	3.05	1.0
	Theory, twisted	3.35	2.88	3.2	3.5
	Theory, planar	3.07	2.79	3.4	3.7
5	Experiment	3.28	2.87	3.6	3.4	3.05	3.00	0.75
	Theory	3.27	2.85	3.6	3.8
8	Theory, twisted	3.17	2.82	4.6	4.3
	Theory, planar	2.86	2.69	5.0	4.7
12	Theory, twisted	3.13	2.82	5.5	4.4
	Theory, planar	2.79	2.69	6.4	5.2
n	Exper., twisted	3.19	2.87	...	4.0	3.01	2.98	0.54
	Exper., planar	~2.9	2.77	...	4.8	2.82	2.80	0.45

We also estimated the experimental vertical transition energies E_{vert} for absorption (abs) and emission (em) using³⁹

$$E_{\text{vert}}(\text{abs}) = \int EA(E)dE / \int A(E)dE \quad (4a)$$

and

$$E_{\text{vert}}(\text{em}) = \int EI(E)dE / \int I(E)dE, \quad (4b)$$

where $A(E)$ is the absorbance and $I(E)$ is the fluorescence intensity at the photon energy E . The results are given in Table I. The agreement between theoretical and experimental values is generally within 0.05 eV except for the fluorescence of the dimer and the monomer, where the deviations are 0.08 and 0.3 eV, respectively. The origin of the discrepancy for the monomer is currently unknown but is in agreement with earlier work.²⁸

Theoretically we also investigated a series of planar backbone oligofluorenes with 4, 8, and 12 fluorene units, respectively. For a single molecule, the planar backbone conformation is not stable but needs to be stabilized externally, which can, for example, occur in a solid-state environment. However, if calculations are started from an initially planar chain conformation, the geometry can be optimized without destroying planarity and, subsequently, transition energies and transition dipoles for the planar backbone conformation can be calculated. Transition energies for the planar backbone conformation (β -phase) are lower than for the twisted backbone (α -phase) in good agreement with previous experimental observations.¹⁸⁻²³ Transition dipoles for the planar backbone conformation are larger by about 20% than for the twisted conformation both in theory and experiment. Experimental fluorescence dipoles found in PFO are very similar to the calculated values for the longest oligomers in both conformations, which indicates that the effective conjugation length in PFO is between 8 and 12 repeat units. This is consistent with the estimate of 12 repeat units obtained from the trend in the transition energy.²⁶ The extent of excited state delocalization can be lower than the effective conjugation length and is discussed in the next section.

B. Exciton self-trapping and molecular conformations

Figure 4 shows the transition dipoles as a function of oligomer length on a logarithmic scale. The absorption dipoles on this scale roughly follow an approximately linear dependence for $2 \leq n \leq 12$ with a slope of 0.5, which implies an $n^{0.5}$ dependence on the number of repeat units n . Slightly higher values of the exponent of 0.6 and 0.7 were reported previously for shorter oligomers (up to seven repeat units).^{29,31} The transition dipole for fluorescence also follows the $\sim n^{0.5}$ dependence but only for $2 \leq n \leq 5$, whereas for longer chains the growth of the transition dipole is much weaker.

In Fig. 5 the change in single-particle electron density upon photoexcitation is visualized both for S_0 (absorption) and S_1 (fluorescence) equilibrium molecular geometries for the longest oligomers (12 fluorene units) studied. While the excitation in absorption is clearly extended over most of the

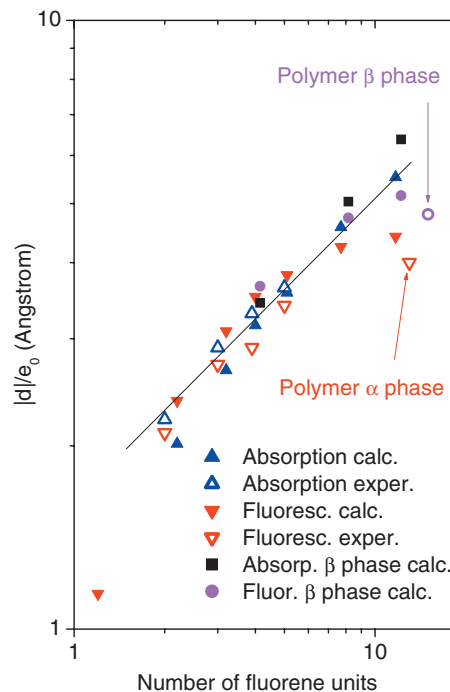


FIG. 4. Transition dipole vs oligomer length on a double logarithmic plot. The solid line shows a fit to the $\propto n^{0.5}$ dependence of the absorption dipole for $n \geq 2$.

molecules' length, it is much more localized in the middle of the oligomer in fluorescence. This behavior is attributed to structural relaxation of the molecules in the excited state leading to localization of the excitation (exciton self-trapping). Both changes in bond-length alternation and changes in interfluorene-unit dihedral angles can contribute to the self-trapping effect.^{27,40-44} We note that although we choose to visualize the excitations by difference densities to which (due to electronic correlations) multiple molecular orbitals contribute, a very similar picture of the self-trapping can be obtained from the spatial extent of the highest occupied molecular orbital (HOMO) and lowest unoccupied molecular orbital (LUMO) for the respective S_0 and S_1 geometries.

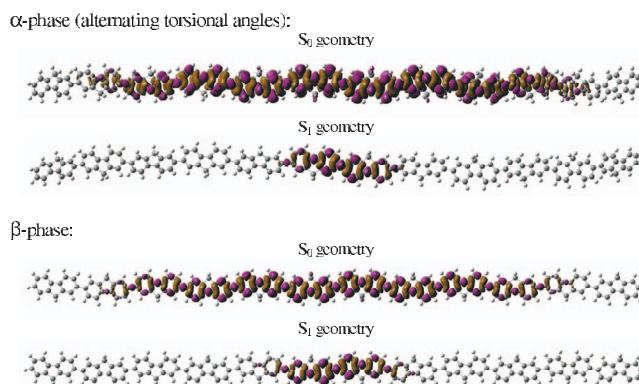


FIG. 5. Visualization of the change in the single-particle electron density upon photoexcitation for twisted (α -phase) and planar (β -phase) chain conformations. Shown are isosurfaces (at 9% of the maximum value) of the difference of SCF density and CIS density of the first excited singlet state. The data are obtained from a single-point CIS calculation for the optimized S_0 (absorption) and S_1 (fluorescence) molecular geometries, respectively.

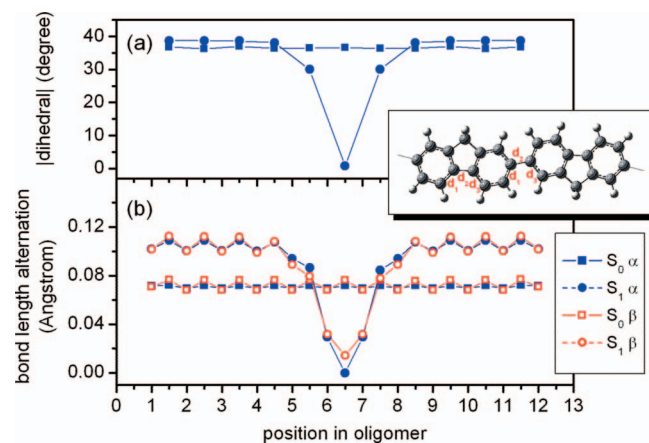


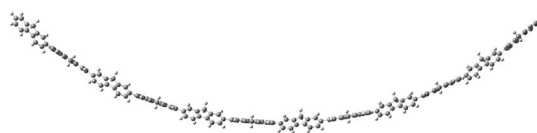
FIG. 6. (a) Dihedral angle between adjacent fluorene units. (b) Bond length alternation $d_2 - (d_1 + d_3)/2$ along the oligomer chain. [(a) and (b)] Results are shown for oligomers with 12 fluorene repeat units in the electronic ground state, S_0 , and first excited singlet state, S_1 , optimized geometries for α - and β -phase conformations, respectively. Dihedrals for the β -phase are all equal zero (not shown).

In support of the previous discussion on self-trapping of the excitation in the excited state equilibrium geometry, Fig. 6 shows the bond length alternation defined as $d_2 - (d_1 + d_3)/2$ (same definition as in Ref. 27) for the molecules shown in Fig. 5. In the excited state equilibrium geometry, the bond length alternation is substantially reduced around the center of the chain corresponding to the region where self-trapping occurs (compare Fig. 5).

Beyond visualization of the self-trapping of excitations, Figs. 5 and 6 are also helpful in interpreting some details of the data shown in Fig. 4. The fluorescence transition dipole saturates faster with increasing oligomer length than the absorption transition dipole. This can be understood as follows. Figure 5 indicates that in fluorescence the excitation is localized (“trapped”) in the middle of the molecule, whereas in absorption it is extended all the way to the boundaries of the molecule, even for the longest oligomer studied. Due to the smaller spatial extent of the excitation in fluorescence, a certain critical length is reached earlier, beyond which making the molecule longer affects the transition energies and transition dipoles only slightly. This critical length corresponds to about five fluorene units (Fig. 4). In absorption, even for the longest chains considered, the saturation length has not been reached in this study and the excitations are still influenced by the boundaries of the molecules.

All of the data discussed above have been calculated for molecular conformations where interfluorene-unit dihedral angles are finite (α -phase) and alternate while going along the chain. However, going beyond the dimer in oligomer length, the definition of the α -phase is no longer unique, and different molecular conformations can be realized. In the following, we briefly address this issue based on a discussion of the two extreme scenarios, where dihedral angles between adjacent units change sign while going along the oligomer chain [twisting the fluorene units back and forth, Fig. 7(a)], or have the same sign along the entire chain [resulting in a helix-like structure of the molecule, Fig. 7(b)]. We note that these two limiting cases are both equally unlikely to be real-

(a) α -phase, alternating torsional angles:



(b) α -phase, helix geometry:



FIG. 7. Electronic ground state equilibrium geometries for oligomers with finite interunit dihedral angles (α -phase) with 12 fluorene repeat units. Shown are the two extreme scenarios, where dihedral angles between adjacent units (a) change sign while going along the chain (twisting the fluorene units back and forth), or (b) have the same sign along the entire chain (resulting in a helix-like structure).

ized because they both represent highly ordered conformations. However, studying these extremes gives a feeling for what role conformational variations may play in a real system. In Fig. 7 we show the conformations that are assumed by the molecules after geometry optimization. Optimization for both molecules was done with an initially straight (not bent) structure but with alternating and continuous interunit dihedral angles, respectively. While the helix conformation stays straight, the molecule with alternating dihedral angles assumes a strongly bent equilibrium geometry. Apart from these significant differences in shape, the transition dipole from ground to first excited singlet state is $\sim 6\%$ bigger for the helix than for the alternating twist conformation. The transition energies differ by an insignificant 6 meV. The conformational dependence of these quantities is found to be less pronounced for the shorter oligomers investigated.

In Fig. 5 the change in single-particle electron density upon photoexcitation is also visualized for the β -phase oligomer with 12 fluorene units. As shown in the figure, the observed self-trapping of the excitation in the S_1 equilibrium geometry is very similar in the calculations for planar (β -phase) and twisted (α -phase) chain conformations. This indicates that it occurs primarily due to a decrease in the bond-length alternation in the excited state; changes in the dihedral angles play only a minor role for the self-trapping found here. Figure 6 confirms that the reduction in bond length alternation for the two phases (α and β) is indeed very similar. In contrast with what might have been expected,²³ self-trapping is found to be only marginally less pronounced in the planar conformation. However, this small conformational difference in self-trapping still explains the slightly slower saturation of fluorescence transition dipole in Fig. 3(a) with oligomer length for the β -phase than for the α -phase. For both α - and β -phase oligomers, the fluorescence transition dipole is found to saturate significantly faster with increasing oligomer length than the absorption transition dipole.

C. Periodic boundary conditions

To complete the previous discussion on saturation of transition energies and transition dipoles with chain length, we mimic the case of a fluorene polymer by using PBCs in the geometry optimizations in the electronic ground state.

(a) α -phase, PBC S_0 geometry:(b) β -phase, PBC S_0 geometry:

(c)

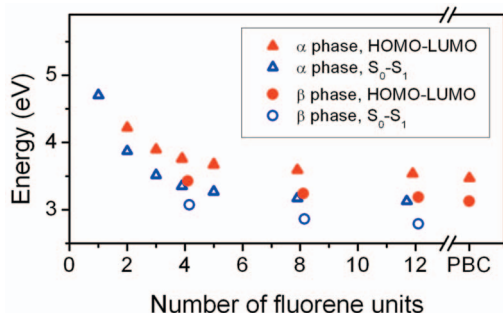


FIG. 8. [(a) and (b)] Molecular structures optimized with PBCs. Results are shown for finite (resembling α -phase polyfluorene) and zero (resembling β -phase polyfluorene) dihedral angle between adjacent fluorene units. (c) Single-particle energy gap (difference of HOMO and LUMO Kohn-Sham orbital energies) shown as solid symbols for the electronic ground state, S_0 , optimized geometry. Results are given for oligomers of finite length and for calculations using PBCs, resembling the polymer with infinite number of fluorene units. For the oligomers also the TD-DFT transition energies (open symbols) are shown for comparison.

For the simplest case of a one-dimensional periodic fluorene-based system, where the unit cell contains only two fluorene units, there are two obvious scenarios. The first case resembles the α -phase polymer with alternating dihedral angles between adjacent fluorene units discussed above, and the second resembles the β -phase polymer. The optimized ground state geometries are shown in Figs. 8(a) and 8(b). Figure 8(c) shows the single particle energy gap, the minimum energy difference between lowest unoccupied crystal orbital and highest occupied crystal orbital, obtained from these calculations together with the corresponding energy gap calculated for the oligomers (energy difference between LUMO and HOMO). First, comparing the oligomer data with the correlated TD-DFT transition energies in Fig. 3(b), we note that the actual “exciton” transition is expected to be about 0.5 eV lower than the single-particle energy gap. The calculations with PBCs yield a single-particle energy gap ~ 0.06 eV lower than the one for the finite-length oligomer with 12 repeat units. We note that the strongly bent molecular conformation in Fig. 7 is in contrast with the straight PBC structure in Fig. 8 (which represents the case of alternating dihedrals). Therefore, the PBC scenario in this case does not quite resemble the behavior of an isolated single fluorene oligomer chain; however, our results indicate that the transition energies can be very similar.

IV. CONCLUSIONS

We theoretically and experimentally investigated optical transitions between the ground and the lowest energy singlet excited state in fluorene oligomers. Good agreement was

found between experiment and theory for transition energies and transition dipoles and it was shown that the finite fluorescence QY needs to be considered in the determination of transition dipoles in fluorescence. DFT calculations have been extended to longer oligomer chains (up to 12 units) than previously studied to investigate saturation of transition energies and transition dipoles with increasing oligomer length. We find that saturation occurs at shorter oligomer lengths for transition dipoles deduced from fluorescence than for those deduced from absorption. This difference indicates the importance of exciton self-trapping in fluorene oligomers and polymers. The calculations show very similar exciton self-trapping for the twisted and planar backbone conformations of oligofluorenes, which indicates that it occurs primarily due to a decrease in bond-length alternation in the relaxed geometry of the excited state. For the twisted oligofluorene backbone, different molecular conformations were also studied theoretically. The ground state conformation of the twisted backbone fluorene oligomer with 12 repeat units is found to be dependent on changes in the alternation of interfluorene-unit dihedral angles. A helix and an alternating-twist structure, which show significantly different molecular equilibrium geometries, have been studied. For these two extreme cases, the difference in conformation yields a small difference (6%) in the transition dipoles and almost no change in transition energies. We also reported the first DFT calculations for twisted and planar backbone polyfluorenes using periodic boundary conditions.

ACKNOWLEDGMENTS

We are grateful to the Engineering and Physical Sciences Research Council for financial support.

- ¹ *Polyfluorenes*, edited by U. Scherf and D. Neher (Springer, Berlin, 2008).
- ² Y. Ohmori, M. Uchida, K. Muro, and K. Yoshino, *Jpn. J. Appl. Phys.*, Part 2 **30**, L1941 (1991).
- ³ Q. Pei and Y. Yang, *J. Am. Chem. Soc.* **118**, 7416 (1996).
- ⁴ M. Grell, X. Long, D. D. C. Bradley, M. Inbasekaran, and E. P. Woo, *Adv. Mater. (Weinheim, Ger.)* **9**, 798 (1997).
- ⁵ A. W. Grice, D. D. C. Bradley, M. T. Bernius, M. Inbasekaran, W. W. Wu, and E. P. Woo, *Appl. Phys. Lett.* **73**, 629 (1998).
- ⁶ L. L. Chua, J. Zaumseil, J.-F. Chang, E. C.-W. Ou, P. K.-H. Ho, H. Sirringhaus, and R. H. Friend, *Nature (London)* **434**, 194 (2005).
- ⁷ R. Schroeder, B. Ullrich, W. Graupner, and U. Scherf, *J. Phys.: Condens. Matter* **13**, L313 (2001).
- ⁸ Y. Morel, A. Irimia, P. Najechalski, Y. Kervella, O. Stephan, P. L. Baldeck, and C. Andraud, *J. Chem. Phys.* **114**, 5391 (2001).
- ⁹ H. Sirringhaus, R. J. Wilson, R. H. Friend, M. Inbasekaran, W. W. Wu, E. P. Woo, M. Grell, and D. D. C. Bradley, *Appl. Phys. Lett.* **77**, 406 (2000).
- ¹⁰ M. Ahles, A. Hepp, R. Schmechel, and H. von Seggern, *Appl. Phys. Lett.* **84**, 428 (2004).
- ¹¹ M. N. Shkunov, R. Österbacka, A. Fujii, K. Yoshino, and Z. V. Vardeny, *Appl. Phys. Lett.* **74**, 1648 (1999).
- ¹² M. Theander, T. Granlund, A. Ruseckas, V. Sundström, D. M. Johansson, M. R. Andersson, and O. Inganäs, *Adv. Mater. (Weinheim, Ger.)* **13**, 323 (2001).
- ¹³ G. Heliotis, R. Xia, D. D. C. Bradley, G. A. Turnbull, I. D. W. Samuel, P. Andrew, and W. L. Barnes, *Appl. Phys. Lett.* **83**, 2118 (2003).
- ¹⁴ Y. Yang, G. A. Turnbull, and I. D. W. Samuel, *Appl. Phys. Lett.* **92**, 163306 (2008).
- ¹⁵ D. Amarasinghe, A. Ruseckas, A. Vasdekis, G. A. Turnbull, and I. D. W. Samuel, *Adv. Mater. (Weinheim, Ger.)* **21**, 107 (2009).
- ¹⁶ G. Lieser, M. Oda, T. Miteva, A. Meisel, H.-G. Nothofer, U. Scherf, and D. Neher, *Macromolecules* **33**, 4490 (2000).

- ¹⁷N. Godbert, P. L. Burn, S. Gilmour, J. P. J. Markham, and I. D. W. Samuel, *Appl. Phys. Lett.* **83**, 5347 (2003).
- ¹⁸M. Grell, D. D. C. Bradley, G. Ungar, J. Hill, and K. S. Whitehead, *Macromolecules* **32**, 5810 (1999).
- ¹⁹M. Ariu, M. Sims, M. D. Rahn, J. Hill, A. M. Fox, D. G. Lidzey, M. Oda, J. Cabanillas-Gonzales, and D. D. C. Bradley, *Phys. Rev. B* **67**, 195333 (2003).
- ²⁰J. Peet, E. Brocker, Y. H. Xu, and G. C. Bazan, *Adv. Mater. (Weinheim, Ger.)* **20**, 1882 (2008).
- ²¹W. C. Tsoi, A. Charas, A. J. Cadby, G. Khalil, A. M. Adawi, A. Iraqi, B. Hunt, J. Morgado, and D. G. Lidzey, *Adv. Funct. Mater.* **18**, 600 (2008).
- ²²K. Becker and J. M. Lupton, *J. Am. Chem. Soc.* **127**, 7306 (2005).
- ²³E. Da Como, K. Becker, J. Feldmann, and J. M. Lupton, *Nano Lett.* **7**, 2993 (2007).
- ²⁴P. Prins, F. C. Grozema, B. S. Nehls, T. Farrell, U. Scherf, and L. D. A. Siebbeles, *Phys. Rev. B* **74**, 113203 (2006).
- ²⁵C. Rothe, F. Galbrecht, U. Scherf, and A. Monkman, *Adv. Mater. (Weinheim, Ger.)* **18**, 2137 (2006).
- ²⁶G. Klaerner and R. D. Miller, *Macromolecules* **31**, 2007 (1998).
- ²⁷I. Franco and S. Tretiak, *J. Am. Chem. Soc.* **126**, 12130 (2004).
- ²⁸E. Jansson, P. C. Jha, and H. Ågren, *Chem. Phys.* **336**, 91 (2007).
- ²⁹R. Anemian, J.-C. Mulatier, C. Andraud, O. Stefan, and J.-C. Vial, *Chem. Commun. (Cambridge)* 1608 (2002).
- ³⁰D. Wasserberg, S. P. Dudek, S. C. J. Meskers, and R. A. J. Janssen, *Chem. Phys. Lett.* **411**, 273 (2005).
- ³¹C. Chi, C. Im, and G. Wegner, *J. Chem. Phys.* **124**, 024907 (2006).
- ³²A. L. Kanibolotsky, R. Berridge, P. J. Skabara, I. F. Perepichka, D. D. C. Bradley, and M. Koeberg, *J. Am. Chem. Soc.* **126**, 13695 (2004).
- ³³R. S. Knox and H. van Amerongen, *J. Phys. Chem. B* **106**, 5289 (2002).
- ³⁴Solvent shrinkage is estimated assuming the volume thermal expansion coefficient of $1.26 \times 10^{-4} \text{ K}^{-1}$, http://terathane.invista.com/doc/files/781/thf_data_sheet.pdf.
- ³⁵K. I. Igumenshchev, S. Tretiak, and V. Y. Chernyak, *J. Chem. Phys.* **127**, 114902 (2007).
- ³⁶F. B. Dias, J. Morgado, A. L. Macanita, F. P. da Costa, H. D. Burrows, and A. P. Monkman, *Macromolecules* **39**, 5854 (2006).
- ³⁷S. J. Strickler and R. A. Berg, *J. Chem. Phys.* **37**, 814 (1962).
- ³⁸U. Rant, U. Scherf, M. Rehahn, P. Galda, J. L. Brédas, and E. Zojer, *Synth. Met.* **127**, 241 (2002).
- ³⁹J. Gierschner, J. Cornil, and H.-J. Egelhaaf, *Adv. Mater. (Weinheim, Ger.)* **19**, 173 (2007).
- ⁴⁰S. Tretiak, A. Saxena, R. L. Martin, and A. R. Bishop, *Phys. Rev. Lett.* **89**, 097402 (2002).
- ⁴¹S. Kilina, E. R. Batista, P. Yang, S. Tretiak, A. Saxena, R. L. Martin, and D. L. Smith, *ACS Nano* **2**, 1381 (2008).
- ⁴²S. Karabunarliev and E. B. Bittner, *J. Chem. Phys.* **118**, 4291 (2003).
- ⁴³E. Hennebicq, C. Deleener, J. L. Brédas, G. D. Scholes, and D. Beljonne, *J. Chem. Phys.* **125**, 054901 (2006).
- ⁴⁴A. Ruseckas and I. D. W. Samuel, *Phys. Status Solidi C* **3**, 263 (2006).